

# ***Supporting Information for***

## **Enhanced Sulfate Formation in Mixed Biomass Burning and Sea-salt Particles Mediated by Photosensitization: Effects of Chloride and Nitrogen-containing Compounds**

Rongzhi Tang<sup>1,2</sup>, Jialiang Ma<sup>3</sup>, Ruifeng Zhang<sup>4</sup>, Weizhen Cui<sup>1</sup>, Yuanyuan Qin<sup>5</sup>, Yangxi Chu<sup>6</sup>, Yiming Qin<sup>1</sup>, Alexander L. Vogel<sup>3</sup>, Chak K. Chan<sup>4,\*</sup>

<sup>1</sup> School of Energy and Environment, City University of Hong Kong, Hong Kong, China

<sup>2</sup> Shenzhen Research Institute, City University of Hong Kong, Shenzhen 518057, China

<sup>3</sup> Institute for Atmospheric and Environmental Sciences, Goethe-University Frankfurt, 60438 Frankfurt am Main, Germany

<sup>4</sup> Division of Physical Science and Engineering, King Abdullah University of Science and Technology (KAUST), Thuwal 23955-6900, Kingdom of Saudi Arabia

<sup>5</sup> College of Resources and Environment, University of Chinese Academy of Sciences, Beijing, 100049, China

<sup>6</sup> State Key Laboratory of Environmental Criteria and Risk Assessment, Chinese Research Academy of Environmental Sciences, Beijing, 100012, China

*Correspondence to:* Chak K. Chan (chak.chan@kaust.edu.sa)

## Table of Contents

**Text S1** Chemical analysis

**Text S2** Possible pathways involved in the  $\text{SO}_2/\text{HSO}_3^-$  oxidation

**Table S1** Chemical compositions in extracted BB and IS extracts.

**Table S2** Possible photosensitizers, formulas and structures in BB extracts detected by state-of-art mass spectrometer.

**Table S3** Possible acids and formula in BB extracts by ESI- mode. Note that the acids listed appeared at least in six BB extracts.

**Figure S1** Differences of normalized  $\text{SO}_2$  uptake coefficients  $n\gamma_{\text{SO}_2}$  between fresh and aged BB-NaCl droplets.

**Figure S2** Correlation of (a) Fe and (b) Mn concentration with normalized  $\text{SO}_2$  uptake coefficient ( $n\gamma_{\text{SO}_2}$ )

**Figure S3** Contributions of direct and indirect PS\* oxidation to sulfate

**Figure S4** Sulfate production under different droplet compositions (fresh or aged BB-NaCl) as a function of time: (a)  $\text{RS}_{\text{F/A}}$ -NaCl droplets; (b)  $\text{WS}_{\text{F/A}}$ -NaCl droplets; (c)  $\text{CS}_{\text{F/A}}$ -NaCl droplets; (d)  $\text{IS}_{\text{F/A}}$  droplets.

**Figure S5** The intensity contribution (%) of each compound category to the total detected compound intensity: (a)  $\text{RS}_{\text{F}}$ ; (b)  $\text{WS}_{\text{F}}$ ; (c)  $\text{CS}_{\text{F}}$ ; (d)  $\text{IS}_{\text{F}}$ ; (e)  $\text{RS}_{\text{A}}$ ; (f)  $\text{WS}_{\text{A}}$ ; (g)  $\text{CS}_{\text{A}}$ ; (h)  $\text{IS}_{\text{A}}$  by ESI- mode.

**Figure S6** The intensity contribution (%) of each compound category to the total detected compound intensity: (a)  $\text{RS}_{\text{F}}$ ; (b)  $\text{WS}_{\text{F}}$ ; (c)  $\text{CS}_{\text{F}}$ ; (d)  $\text{IS}_{\text{F}}$ ; (e)  $\text{RS}_{\text{A}}$ ; (f)  $\text{WS}_{\text{A}}$ ; (g)  $\text{CS}_{\text{A}}$ ; (h)  $\text{IS}_{\text{A}}$  by ESI+ mode.

**Figure S7** Concentration changes of (a)(b) sulfate and (c)(d) bisulfite using different BB extracts as a function of time, in which (a)(c) represent the results of fresh BB extracts, and (b)(d) represent the results of aged BB extracts.

**Figure S8** Van Krevelen plots of N-bases in (a)  $\text{RS}_{\text{F}}$  and (b)  $\text{RS}_{\text{A}}$ . The color bar represents the double bond equivalent, and the text marker denotes the nitrogen number in each assigned formula. Points that share the same number of nitrogen atoms and are positioned in a linear arrangement belong to identical homologous series based on  $\text{CH}_2$ . These series are characterized by a core molecule combined with  $(\text{CH}_2)_n$  units, where n is equal to or greater than zero.

**Figure S9** Heat map of Pearson correlations between sulfate formation rate (k) and other factors, including chloride, Fe, Mn, sulfate, nitrate, and different chemical species detected by ESI (-) and ESI (+) mode. Note that the calculations were base on the sulfate formation rate and the original concentrations of the influencing factors in the bulk solution. The symbol  $\times$  indicates non-significance, i.e.,  $p \geq 0.05$ . Red color means positive correlation ( $r > 0$ ), and blue color means negative correlation ( $r < 0$ ). The darker the color, the higher the r value.

**Figure S10.** (a) (b) Sulfate formation and (c) (d) sulfate formation rates by different combinations of PS and chloride: (a)(c) SyrAld-NaCl; (b)(d) VL-NaCl. 1-10, 1-100 and 1-200 represent the mass ratios of different species. Among them, the concentrations of SyrAld and VL were 1 ppm, while the NaCl concentrations were varied, 10, 100 and 200 represent 10 ppm, 100 ppm and 200 ppm, respectively.

**Figure S11** (a) (b) Sulfate formation and (c) (d) sulfate formation rates by different combinations of PS, CHN species and chloride: (a)(c) SyrAld-Pyz-(NaCl); (b)(d) VL-Pyz-(NaCl). 1-1-10, 1-1-100 and 1-1-200 represent the mass ratios of different species. Among them, the concentrations of SyrAld, VL and Pyz were 1 ppm, while the NaCl concentrations were varied, 10, 100 and 200

represent 10 ppm, 100 ppm and 200 ppm, respectively.

**Figure S12** (a) (b) Sulfate formation and (c) (d) sulfate formation rates by different combinations of PS, CHON species and chloride: (a)(c) SyrAld-4-NC-(NaCl); (b)(d) VL-4-NC-(NaCl). 1-1-10, 1-1-100 and 1-1-200 represent the mass ratios of different species. Among them, the concentrations of SyrAld, VL and 4-NC were 1 ppm, while the NaCl concentrations were varied, 10, 100 and 200 represent 10 ppm, 100 ppm and 200 ppm, respectively.

**Figure S13** Chloride concentration as a function of time with different NaCl addition to RS extracts

**Figure S14** Chloride concentration as a function of time with different NaCl addition to PS-(CHN/CHON) system.

## TEXT

### Text S1 Chemical analysis

The sulfate, nitrate and chloride anions in the BB extracts were analyzed by an Dionex ion chromatography (IC, Dionex ICS-1100, Sunnyvale, CA) with a Dionex AS-DV autosampler (Sunnyvale, CA). The key analytical system includes a suppressed conductivity detector (Sunnyvale, CA), a self-regenerating anion suppressor (ASRS 300) and an AS 11 analytical column.

The particulate organic matter collected on BB filters were analyzed by a comprehensive two-dimensional gas chromatography-mass spectrometry (GC×GC-MS, GC-MS TQ 8050, SHIMADZU, Japan) coupled with a thermal desorption module (TDS 3, C506, Gerstel). The first column of GC×GC was non-polar SH-Rxi-1ms (30 m × 0.25 mm × 0.25 μm) and second column was mid-polar BPX50 (2.5 m × 0.1 mm × 0.1 μm). The modulation period was 6 s. The desorption temperature of TDS was 280 °C. More details can be found in previous research.<sup>1</sup> Water-soluble organics of the BB extracts were analyzed by an ultra-high performance liquid chromatography (Thermo Scientific Dionex UltiMate 3000 UHPLC, USA) coupled with high-resolution Orbitrap Fusion Lumos Tribrid mass spectrometry (UHPLC-Orbitrap-HR-MS, Thermo Fisher Scientific, USA). Chromatographic separation was conducted using a reversed-phase column (Acquity HSS T3 column, 100×2.1 mm, 1.8 μm particle size, Waters Corp., Ireland) at 40°C, and the autosampler was cooled at 4 °C. Mobile phases included eluent A (water with 0.1% formic acid) and eluent B (acetonitrile with 0.1% formic acid). The gradient elution program consisted of a 10% B start for 1 min, increasing to 90% B over 25 min, holding for 4 min, decreasing to 10% B in 1 min, and a 5 min re-equilibration. Flow rate was 0.2 mL/min, injection volume was 10 μL. NTA software (Compound Discoverer CD, version 3.2, ThermoFisher Scientific) was employed to identify the chromatographic peak features. Compound identification was based on the combination of features eluting at the same retention time and exhibiting m/z values corresponding to precise mass differences, including isotopes, adducts, clusters, or fragments. In all the experiments, threshold intensities of 1E5 (low) and 1E10 (high) were applied to the two-dimensional coordinate system (RT: 1-20 min, m/z: 50-500). The CD software automatically excluded ions with peak abundances below or above the threshold.

The identified molecular formula, mainly CcHhOoNnSs, were classified into different categories, namely, CHO, CHON, CHONS, CHOS and others. For example, CHON represents compounds composed solely of carbon, hydrogen, oxygen and nitrogen elements. The "others" category includes compounds not falling into CHO, CHON, CHONS, or CHOS, as well as signals without calculated elemental formulas. Molecular formula were also categorized according to their elemental ratios, e.g. H/C, O/C, N/C, double bond equivalents (DBE), modified aromaticity index (AI<sub>mod</sub>) and maximum carbonyl ratio (MCR). The DBE, AI<sub>mod</sub> and MCR<sup>2</sup> were calculated as:

$$DBE=1+c-0.5h+0.5n \quad (1)$$

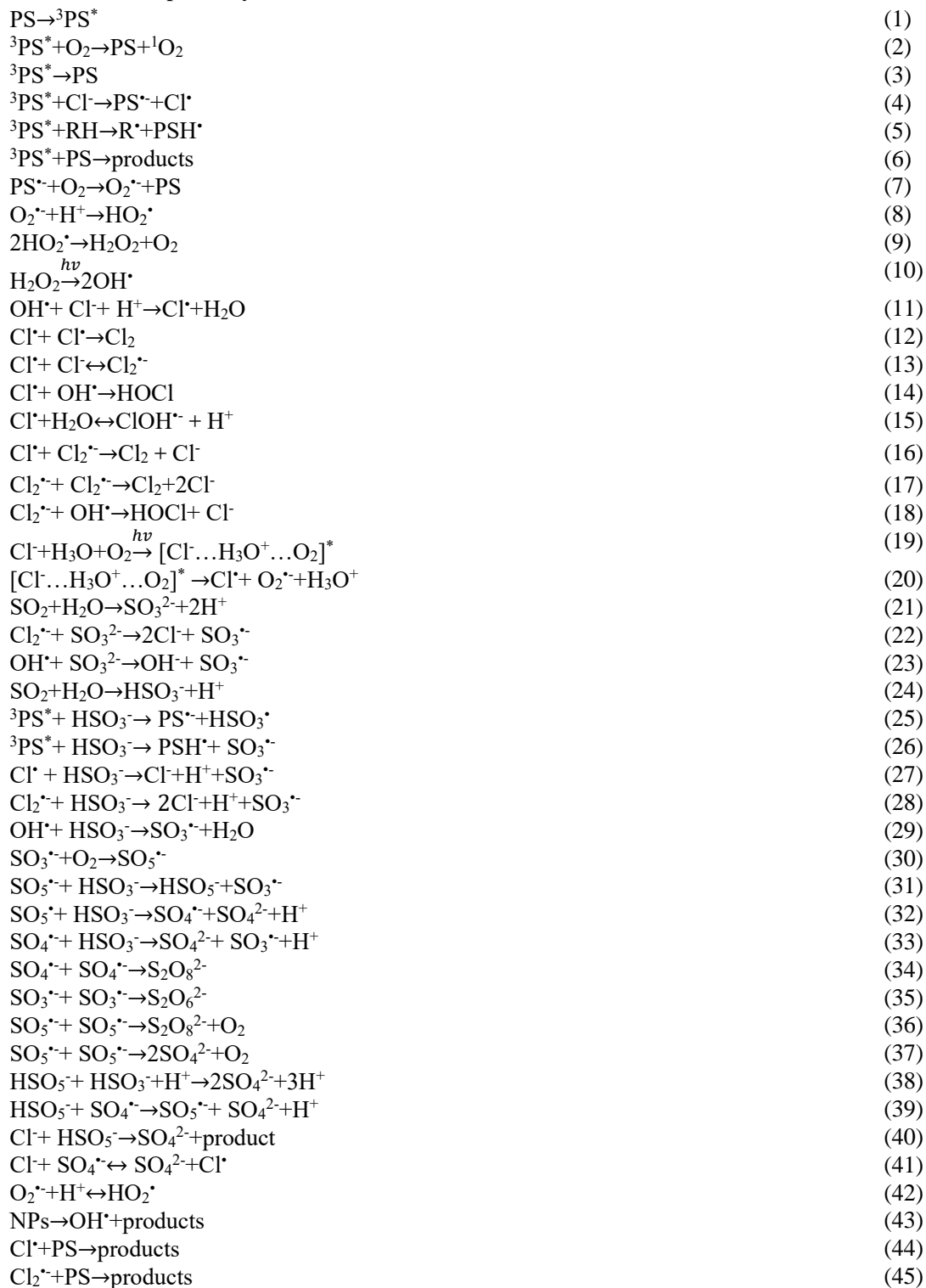
$$AI_{mod}=\frac{DBE_{AI}}{C_{AI}}=\frac{1+c-0.5o-s-0.5(n+h)}{c-0.5o-n-s} \quad (2)$$

$$MCR=\frac{DBE}{o} \quad (3)$$

In which c, h, o and n corresponds to the number of C, H, O and N atoms, respectively in the assigned molecular formula. Formula were categorized into six groups, i.e., condensed aromatics (AI<sub>mod</sub>≥0.67), polyphenolics (0.50 < AI<sub>mod</sub> < 0.67), highly unsaturated and phenolic formula (AI<sub>mod</sub>≤0.5, H/C < 1.5), aliphatics (H/C≥1.5, O/C≤0.9, N=0), peptide-like formula (H/C≥1.5,

O/C≤0.9, N=0) and sugar-like formula (H/C≥1.5, O/C > 0.9).<sup>3,4</sup> For MCR, here we only applied it in CcHhOo compounds. The Equation 3 fits for compounds with larger or equal atom O compared to DBE. If the atom O in CcHhOo is smaller than DBE, then MCR is considered to be 1, i.e., all the O atoms contribute to DBE.

### Text S2 Possible pathways involved in the SO<sub>2</sub>/HSO<sub>3</sub><sup>-</sup> oxidation



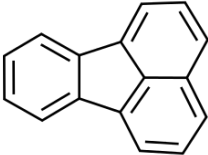
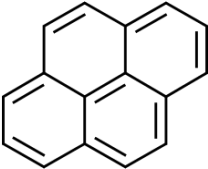
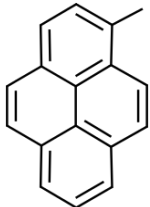
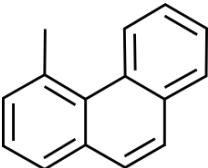
## Tables

Table S1 Chemical compositions in extracted BB and IS extracts.

Category	TOC (mg L <sup>-1</sup> )	Cr (µg L <sup>-1</sup> )	Cu (µg L <sup>-1</sup> )	Fe (µg L <sup>-1</sup> )	Mn (µg L <sup>-1</sup> )	Ni (µg L <sup>-1</sup> )	Ti (µg L <sup>-1</sup> )	Zn (µg L <sup>-1</sup> )	Cl <sup>-</sup> (mg L <sup>-1</sup> )	SO <sub>4</sub> <sup>2-</sup> (mg L <sup>-1</sup> )	NO <sub>3</sub> <sup>-</sup> (mg L <sup>-1</sup> )	∑ <i>anions</i> <sup>a</sup> (mg L <sup>-1</sup> )	∑ <i>anions</i> /TOC
RS <sub>F</sub>	69.9	1.8	0	31.7	5.8	0	73.0	74.5	44.1	6.0	3.2	53.3	0.8
WS <sub>F</sub>	64.5	2.3	4.6	96.9	2.9	1.2	94.2	30.3	41.1	5.2	3.1	49.4	0.8
CS <sub>F</sub>	45.6	0.9	0	31.9	3.5	0	76.9	29.1	9.5	4.5	3.2	17.2	0.4
IS <sub>F</sub>	571.1	1.7	23.2	12.5	7.6	0.7	9.1	77.3	8.1	3.7	5.6	17.5	0.03
RS <sub>A</sub>	61.4	2.6	39.5	87.5	5.2	0.5	76.3	59.5	35.5	5.2	3.1	43.7	0.7
WS <sub>A</sub>	52.7	4.8	31.6	176.7	3.3	1.6	43.7	26.0	39.9	4.9	3.1	47.9	0.9
CS <sub>A</sub>	34.0	2.7	21.8	111.8	3.4	0.5	21.3	26.0	16.9	4.0	3.1	24.0	0.7
IS <sub>A</sub>	584.8	4.2	33.7	87.9	10.1	0.8	17.0	100.1	8.4	4.3	5.6	18.4	0.03

$$\sum \text{anions} = [Cl^-] + [SO_4^{2-}] + [NO_3^-]$$

Table S2 Possible photosensitizers, formulas and structures in BB extracts detected by state-of-art mass spectrometer.

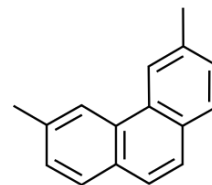
Category	Possible photosensitizers	Formula	Calc. MW	Possible structure	Detected by
PAHs	Fluoranthene	C <sub>16</sub> H <sub>10</sub>	202.256		GC×GC-MS
	Pyrene	C <sub>16</sub> H <sub>10</sub>	202.256		GC×GC-MS
	1-methylpyrene	C <sub>17</sub> H <sub>12</sub>	216.277		GC×GC-MS
	4-methylphenanthrene	C <sub>15</sub> H <sub>12</sub>	192.256		GC×GC-MS

---

3,6-  
dimethylphenanthrene

C<sub>16</sub>H<sub>14</sub>

206.282



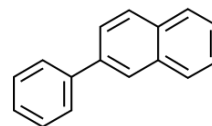
GC×GC-MS

---

2-phenylnaphthalene

C<sub>16</sub>H<sub>12</sub>

204.266



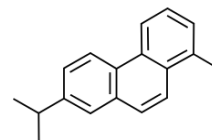
GC×GC-MS

---

Retene

C<sub>18</sub>H<sub>18</sub>

234.335



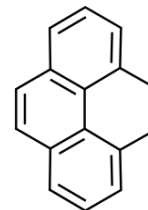
GC×GC-MS

---

4,5-dihdropyrene

C<sub>16</sub>H<sub>12</sub>

204.266



GC×GC-MS

---

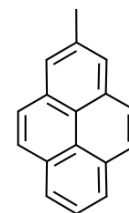


---

2-methylpyrene

C<sub>17</sub>H<sub>12</sub>

216.277



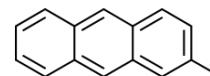
GC×GC-MS

---

2-methylanthracene

C<sub>15</sub>H<sub>12</sub>

192.256



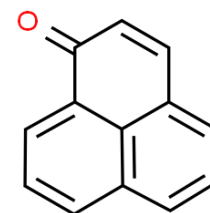
GC×GC-MS

---

1H-Phenalen-1-one

C<sub>13</sub>H<sub>8</sub>O

180.202



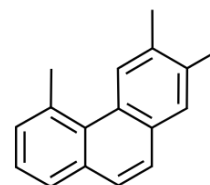
GC×GC-MS

---

2,3,5-  
trimethylphenanthrene

C<sub>17</sub>H<sub>16</sub>

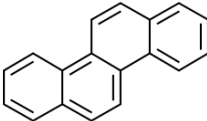
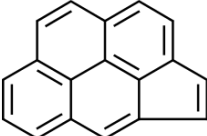
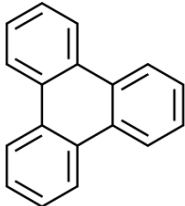
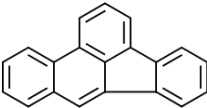
220.309



GC×GC-MS

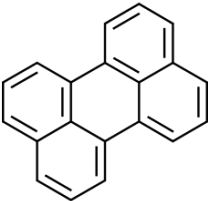
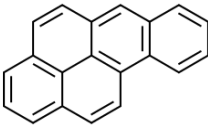
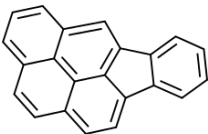
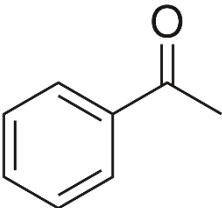
---

---

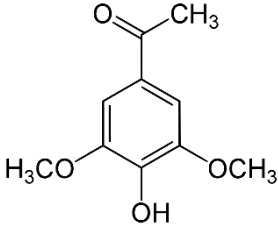
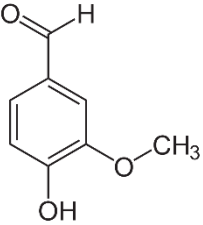
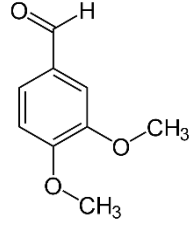
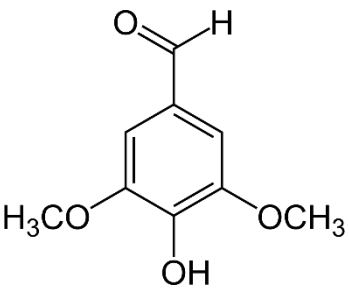
Chrysene	C <sub>18</sub> H <sub>12</sub>	228.288		GC×GC-MS
Cyclopenta[cd]pyrene	C <sub>18</sub> H <sub>10</sub>	226.272		GC×GC-MS
Triphenylene	C <sub>18</sub> H <sub>12</sub>	228.288		GC×GC-MS
Benzo[b]fluoranthene	C <sub>20</sub> H <sub>12</sub>	252.309		GC×GC-MS

---

---

Perylene	C <sub>20</sub> H <sub>12</sub>	252.309		GC×GC-MS
Benzo[a]pyrene	C <sub>20</sub> H <sub>12</sub>	252.309		GC×GC-MS
Indeno[1,2,3-cd]pyrene	C <sub>22</sub> H <sub>12</sub>	276.331		GC×GC-MS
Acetophenone	C <sub>8</sub> H <sub>8</sub> O	120.151		GC×GC-MS UHPLC- Orbitrap-MS (ESI+)

---

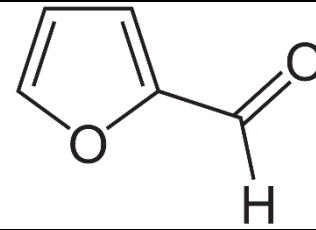
Acetosyringone	C <sub>10</sub> H <sub>12</sub> O <sub>4</sub>	196.202		GC×GC-MS Orbitrap-MS (ESI-)
Vanillin	C <sub>8</sub> H <sub>8</sub> O <sub>3</sub>	152.149		GC×GC-MS Orbitrap-MS (ESI-)
3,4-dimethoxybenzaldehyde	C <sub>9</sub> H <sub>10</sub> O <sub>3</sub>	166.176		GC×GC-MS Orbitrap-MS (ESI-)
Syringaldehyde	C <sub>9</sub> H <sub>10</sub> O <sub>4</sub>	182.17		GC×GC-MS Orbitrap-MS (ESI-)

---

Furfural

C<sub>5</sub>H<sub>4</sub>O<sub>2</sub>

96.08



Orbitrap-MS  
(ESI-)

---

Table S3 Possible acids and formula in BB extracts by ESI- mode. Note that the acids listed appeared at least in six BB extracts.

Possible acids	Formula	Calc. MW
Citraconic acid	C <sub>5</sub> H <sub>6</sub> O <sub>4</sub>	130.0265
Homovanillic acid	C <sub>9</sub> H <sub>10</sub> O <sub>4</sub>	182.0579
Vanillic acid	C <sub>8</sub> H <sub>8</sub> O <sub>4</sub>	168.0423
Succinic acid	C <sub>4</sub> H <sub>6</sub> O <sub>4</sub>	118.0265
3-Methylsalicylic acid	C <sub>8</sub> H <sub>8</sub> O <sub>3</sub>	152.0473
2-Methylbenzoic acid	C <sub>8</sub> H <sub>8</sub> O <sub>2</sub>	136.0524
3,5-Dihydroxybenzoic acid	C <sub>7</sub> H <sub>6</sub> O <sub>4</sub>	154.0266
Salicylic acid	C <sub>7</sub> H <sub>6</sub> O <sub>3</sub>	138.0317
Azelaic acid	C <sub>9</sub> H <sub>16</sub> O <sub>4</sub>	188.1049
Glutaric acid	C <sub>5</sub> H <sub>8</sub> O <sub>4</sub>	132.0422
Sorbic acid	C <sub>6</sub> H <sub>8</sub> O <sub>2</sub>	112.0523
Methylsuccinic acid	C <sub>5</sub> H <sub>8</sub> O <sub>4</sub>	132.0422
3-Allyl-2-hydroxybenzoic acid	C <sub>10</sub> H <sub>10</sub> O <sub>3</sub>	178.063
trans-Cinnamic acid	C <sub>9</sub> H <sub>8</sub> O <sub>2</sub>	148.0524
Ferulic acid	C <sub>10</sub> H <sub>10</sub> O <sub>4</sub>	194.0579
Homogentisic acid	C <sub>8</sub> H <sub>8</sub> O <sub>4</sub>	168.0423
2-Hydroxycinnamic acid	C <sub>9</sub> H <sub>8</sub> O <sub>3</sub>	164.0474
2,3-Dihydro-1-benzofuran-2-carboxylic acid	C <sub>9</sub> H <sub>8</sub> O <sub>3</sub>	164.0473

---

DL-Mandelic acid	C8H8O3	152.0473
6-Methoxysalicylic acid	C8H8O4	168.0423
Isophthalic acid	C8H6O4	166.0266
Phenylglyoxylic acid	C8H6O3	150.0317
4-Hydroxyphenylpyruvic acid	C9H8O4	180.0423
Syringic acid	C9H10O5	198.0529
2-Methylglutaric acid	C6H10O4	146.0579
BMK glycidic acid	C10H10O3	178.063
Caffeic acid	C9H8O4	180.0423
2-Anisic acid	C8H8O3	152.0473
6-Hydroxypicolinic acid	C6H5NO3	139.0269
4-Hydroxymandelic acid	C8H8O4	168.0423
Homovanillic acid	C9H10O4	182.0579
6-Hydroxy-2-naphthoic acid	C11H8O3	188.0474
3-Methoxyphenylacetic acid	C9H10O3	166.063
Sinapinic acid	C11H12O5	224.0685

---

## FIGURES

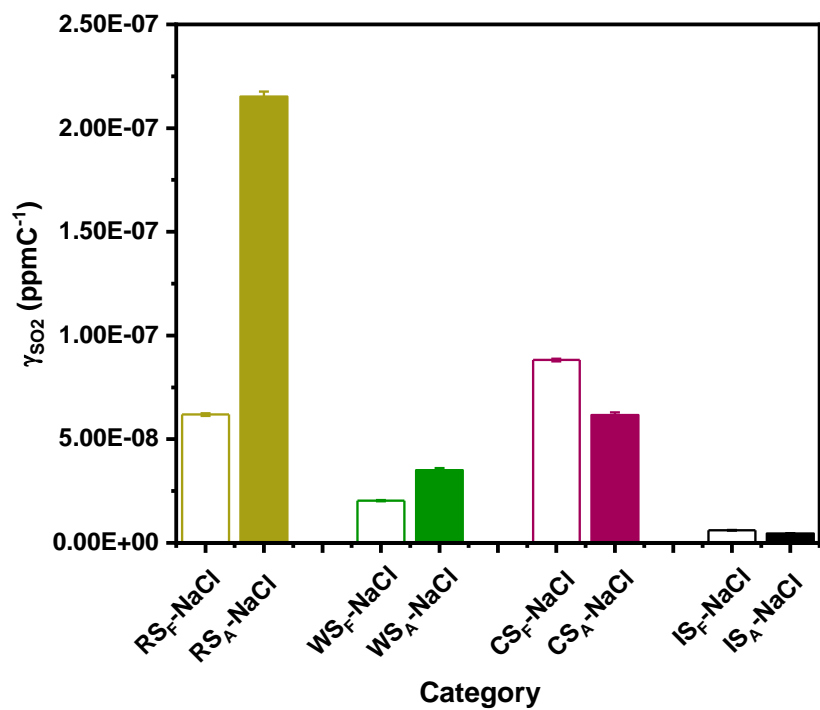


Figure S1 Differences of normalized SO<sub>2</sub> uptake coefficients  $n\gamma_{SO_2}$  between fresh and aged BB-NaCl droplets.



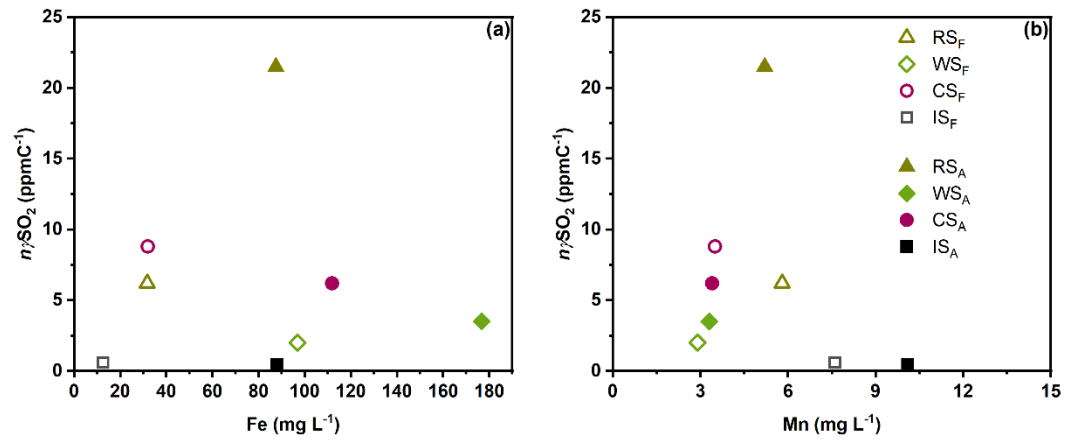
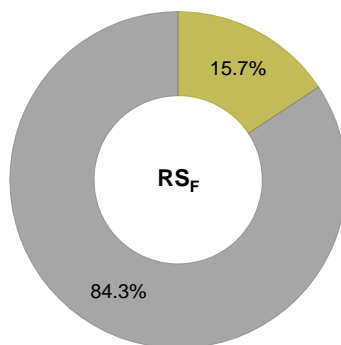
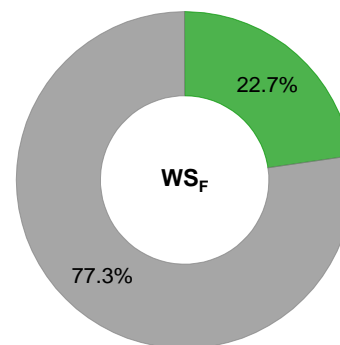


Figure S2 Correlation of (a) Fe and (b) Mn concentration with normalized SO<sub>2</sub> uptake coefficient ( $n\gamma_{SO_2}$ )

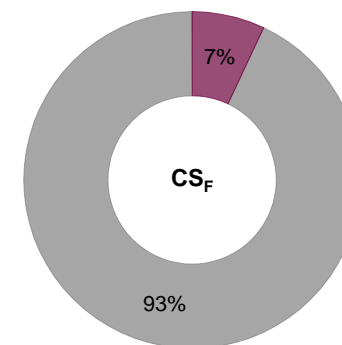
**(a)** Direct RSF\* oxidation  
Indirect RSF\* oxidation



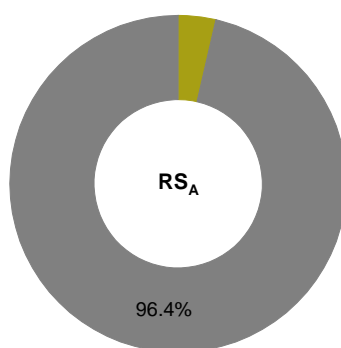
**(b)** Direct WSF\* oxidation  
Indirect WSF\* oxidation



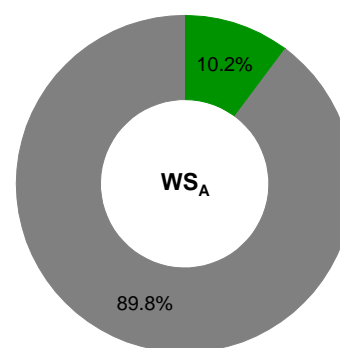
**(c)** Direct CSF\* oxidation  
Indirect CSF\* oxidation



**(d)** Direct RSA\* oxidation  
Indirect RSA\* oxidation



**(e)** Direct WSA\* oxidation  
Indirect WSA\* oxidation



**(f)** Direct CSA\* oxidation  
Indirect CSA\* oxidation

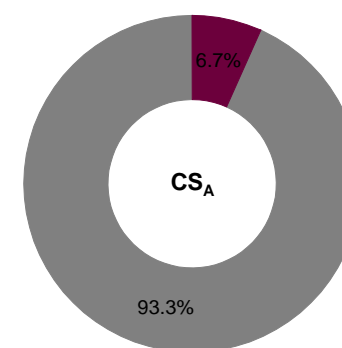


Figure S3 Contributions of direct and indirect PS\* oxidation to sulfate

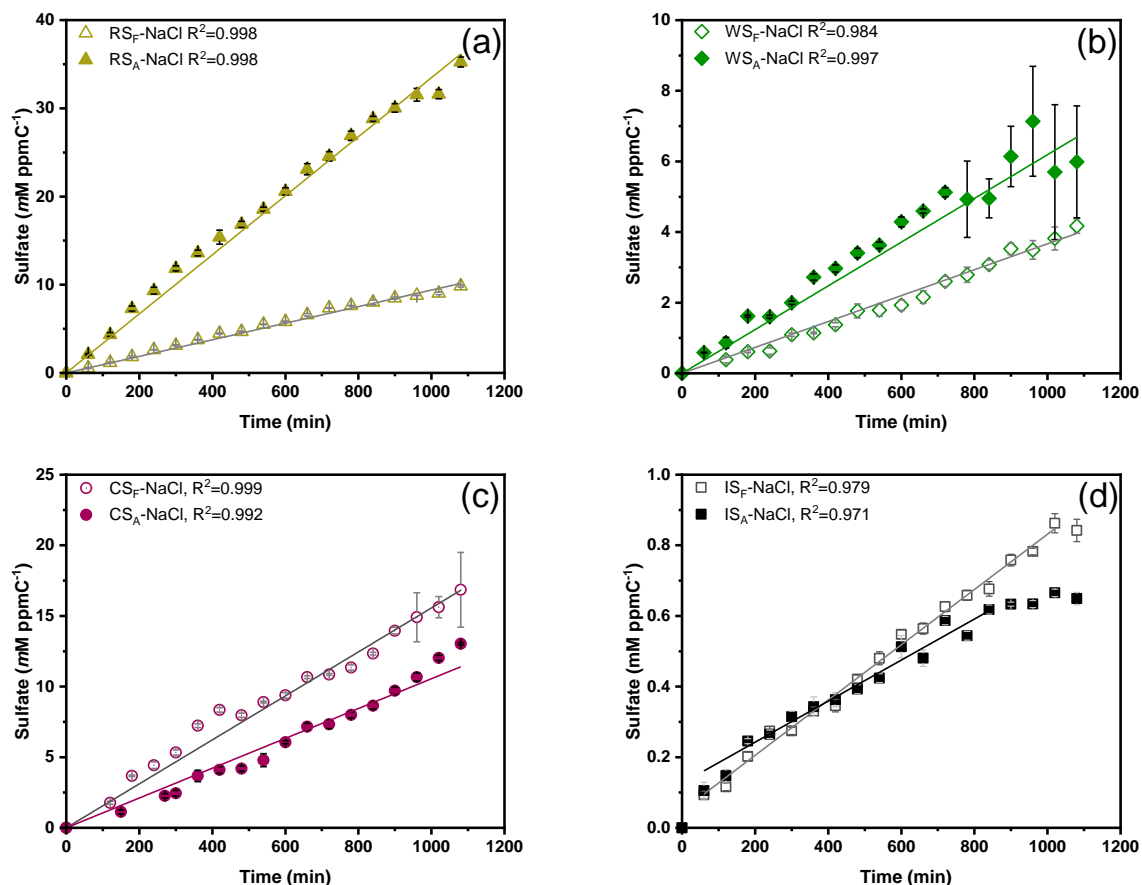


Figure S4 Sulfate production under different droplet compositions (fresh or aged BB-NaCl) as a function of time: (a)  $RS_{F/A}$ -NaCl droplets; (b)  $WS_{F/A}$ -NaCl droplets; (c)  $CS_{F/A}$ -NaCl droplets; (d)  $IS_{F/A}$  droplets.

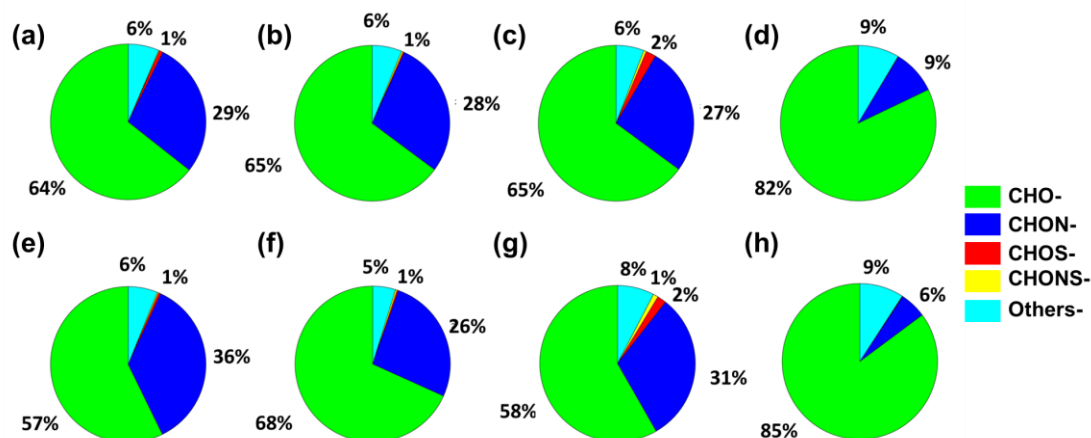


Figure S5 The intensity contribution (%) of each compound category to the total detected compound intensity: (a)  $RS_F$ ; (b)  $WS_F$ ; (c)  $CS_F$ ; (d)  $IS_F$ ; (e)  $RS_A$ ; (f)  $WS_A$ ; (g)  $CS_A$ ; (h)  $IS_A$  by ESI- mode.

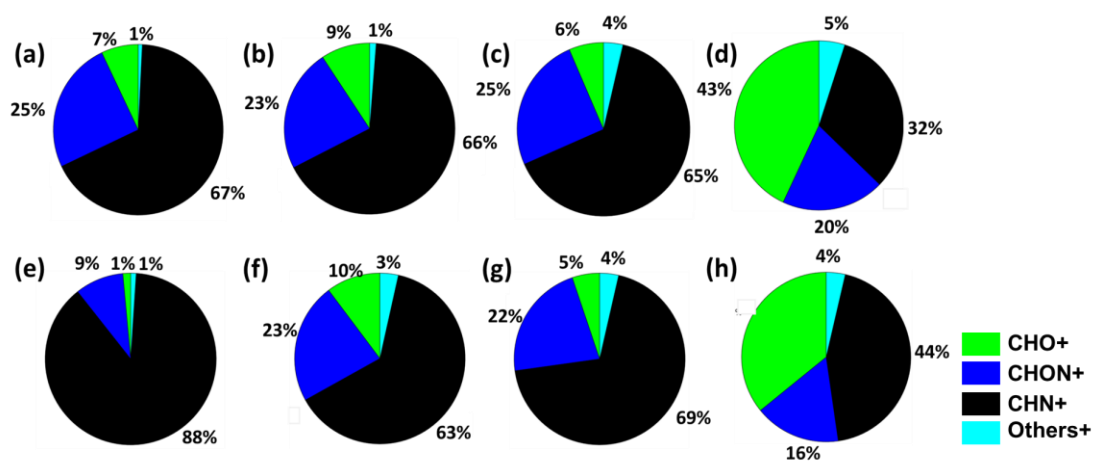


Figure S6 The intensity contribution (%) of each compound category to the total detected compound intensity: (a) RS<sub>F</sub>; (b) WS<sub>F</sub>; (c) CS<sub>F</sub>; (d) IS<sub>F</sub>; (e) RS<sub>A</sub>; (f) WS<sub>A</sub>; (g) CS<sub>A</sub>; (h) IS<sub>A</sub> by ESI+ mode.

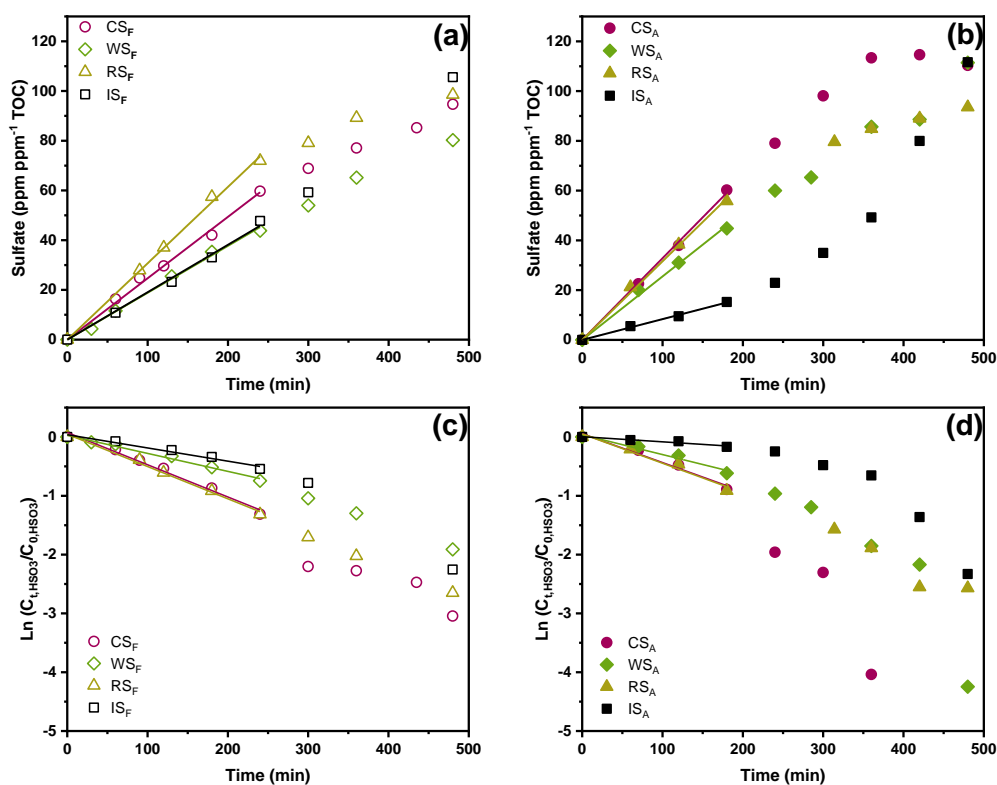


Figure S7 Concentration changes of (a)(b) sulfate and (c)(d) bisulfite using different BB extracts as a function of time, in which (a)(c) represent the results of fresh BB extracts, and (b)(d) represent the results of aged BB extracts.

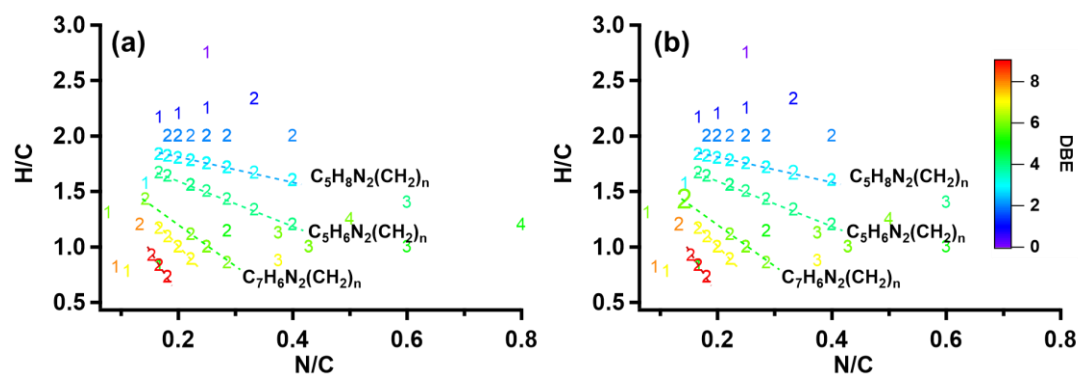
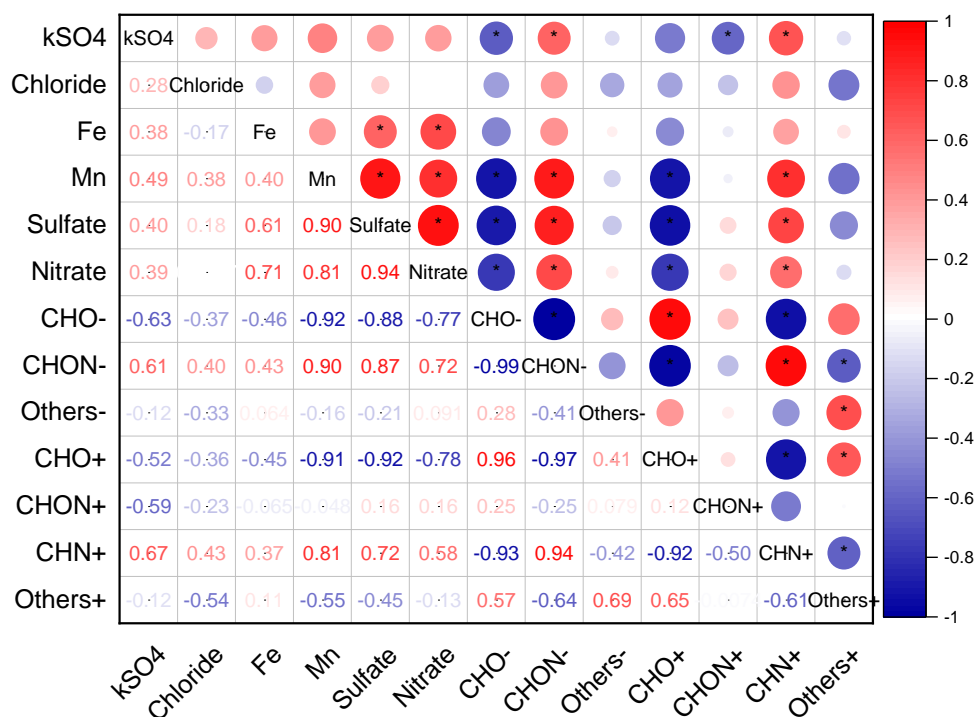


Figure S8 Van Krevelen plots of N-bases in (a)  $RS_F$  and (b)  $RS_A$ . The color bar represents the double bond equivalent, and the text marker denotes the nitrogen number in each assigned formula. Points that share the same number of nitrogen atoms and are positioned in a linear arrangement belong to identical homologous series based on  $CH_2$ . These series are characterized by a core molecule combined with  $(CH_2)_n$  units, where  $n$  is equal to or greater than zero.



\*  $p \leq 0.05$

Figure S9 Heat map of Pearson correlations between sulfate formation rate ( $k$ ) and other factors, including chloride, Fe, Mn, sulfate, nitrate, and different chemical species detected by ESI (-) and ESI (+) mode. Note that the calculations were based on the sulfate formation rate and the original concentrations of the influencing factors in the bulk solution. The symbol \* indicates significance, i.e.,  $p \leq 0.05$ . Red color means positive correlation ( $r > 0$ ), and blue color means negative correlation ( $r < 0$ ). The darker the color, the higher the  $r$  value.

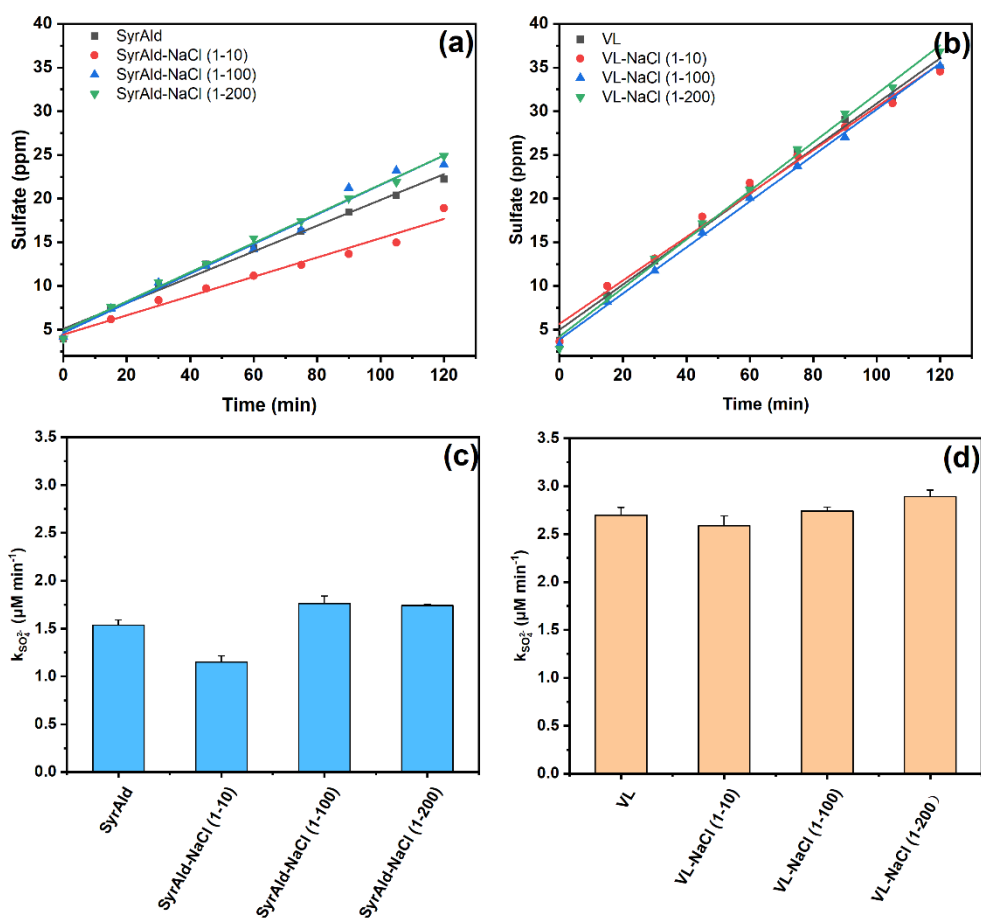


Figure S10. (a) (b) Sulfate formation and (c) (d) sulfate formation rates by different combinations of PS and chloride: (a)(c) SyrAld-NaCl; (b)(d) VL-NaCl. 1-10, 1-100 and 1-200 represent the mass ratios of different species. Among them, the concentrations of SyrAld and VL were 1 ppm, while the NaCl concentrations were varied, 10, 100 and 200 represent 10 ppm, 100 ppm and 200 ppm, respectively.

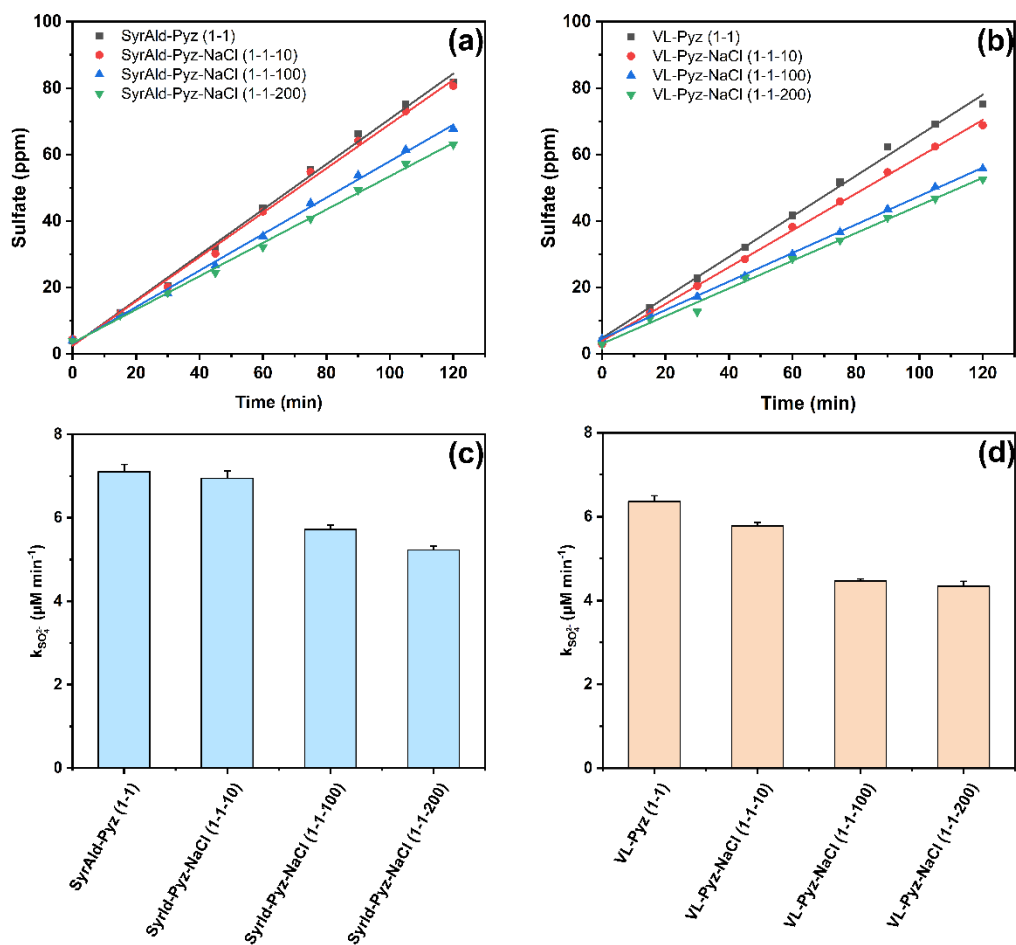


Figure S11. (a) (b) Sulfate formation and (c) (d) sulfate formation rates by different combinations of PS, CHN species and chloride: (a)(c) SyrAld-Pyz-(NaCl); (b)(d) VL-Pyz-(NaCl). 1-1-10, 1-1-100 and 1-1-200 represent the mass ratios of different species. Among them, the concentrations of SyrAld, VL and Pyz were 1 ppm, while the NaCl concentrations were varied, 10, 100 and 200 represent 10 ppm, 100 ppm and 200 ppm, respectively.

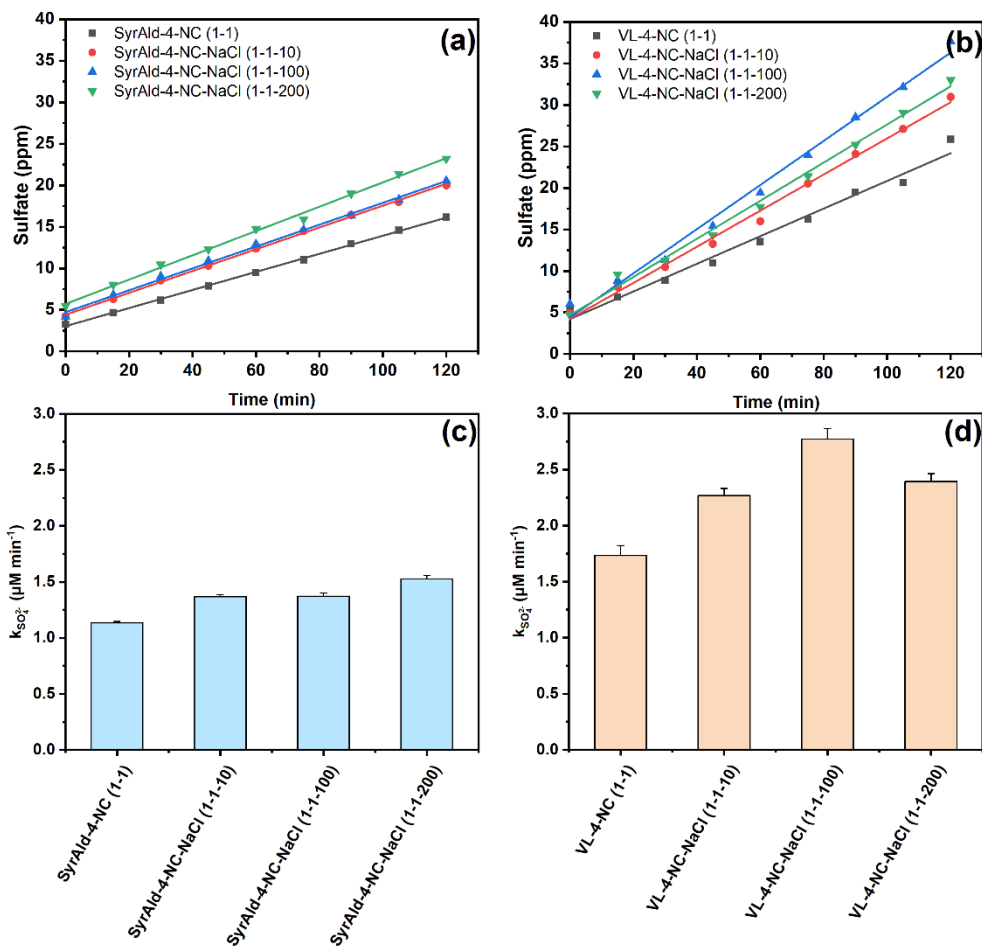


Figure S12. (a) (b) Sulfate formation and (c) (d) sulfate formation rates by different combinations of PS, CHON species and chloride: (a)(c) SyrAld-4-NC-(NaCl); (b)(d) VL-4-NC-(NaCl). 1-1-10, 1-1-100 and 1-1-200 represent the mass ratios of different species. Among them, the concentrations of SyrAld, VL and 4-NC were 1 ppm, while the NaCl concentrations were varied, 10, 100 and 200 represent 10 ppm, 100 ppm and 200 ppm, respectively.



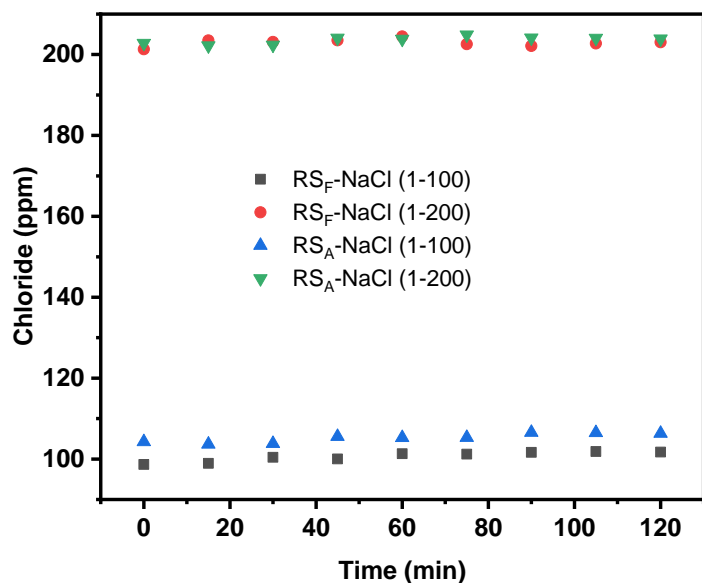


Figure S13. Chloride concentration as a function of time with different NaCl addition to RS extracts

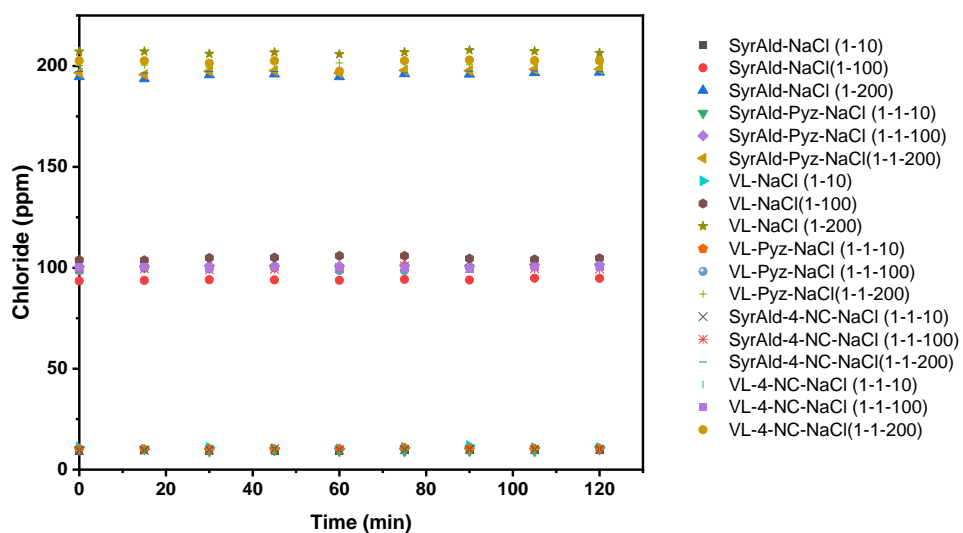


Figure S14. Chloride concentration as a function of time with different NaCl addition to PS-(CHN/CHON) system.

## REFERENCES

- (1) Hu, W.; Zhou, H.; Chen, W.; Ye, Y.; Pan, T.; Wang, Y.; Song, W.; Zhang, H.; Deng, W.; Zhu, M.; et al. Oxidation Flow Reactor Results in a Chinese Megacity Emphasize the Important Contribution of S/IVOCs to Ambient SOA Formation. *Environmental Science & Technology* **2022**, *56* (11), 6880-6893. DOI: 10.1021/acs.est.1c03155.
- (2) Zhang, Y.; Wang, K.; Tong, H.; Huang, R.-J.; Hoffmann, T. The maximum carbonyl ratio (MCR) as a new index for the structural classification of secondary organic aerosol components. *Rapid Communications in Mass Spectrometry* **2021**, *35* (14), e9113. DOI: <https://doi.org/10.1002/rcm.9113>.
- (3) Zherebker, A.; Rukhovich, G. D.; Sarycheva, A.; Lechtenfeld, O. J.; Nikolaev, E. N. Aromaticity Index with Improved Estimation of Carboxyl Group Contribution for Biogeochemical Studies. *Environmental Science & Technology* **2022**, *56* (4), 2729-2737. DOI: 10.1021/acs.est.1c04575.
- (4) Koch, B. P.; Dittmar, T. From mass to structure: An aromaticity index for high-resolution mass data of natural organic matter. *Rapid communications in mass spectrometry* **2006**, *20* (5), 926-932.